Available online at www.sciencedirect.com
ScienceDirect
Bioorganic & Medicinal Chemistry 16 (2008) 3537–3549
Bioorganic & Medicinal Chemistry

N-1*H*-Benzimidazol-5-ylbenzenesulfonamide derivatives as potent hPXR agonists

Cindy Benod,[a] Guy Subra,[a] Virginie Nahoum,[a] Aude Mallavialle,[c] Jean-François Guichou,[a] Julien Milhau,[a] Samuel Roblés,[a] William Bourguet,[a] Jean-Marc Pascussi,[b] Patrick Balaguer[c] and Alain Chavanieu[a,*]

[a]*INSERM, U554, Montpellier, F-34090, Univ Montpellier 1 and 2, CNRS, UMR5048, Centre de Biochimie Structurale, Montpellier F-34090, France*
[b]*INSERM, U632, Montpellier, F-34293, Univ Montpellier 1, Montpellier F-34060, France*
[c]*INSERM, U824, Montpellier, F-34298, Univ Montpellier 1, Montpellier F-34060, France*

Received 10 October 2007; revised 31 January 2008; accepted 8 February 2008
Available online 13 February 2008

Abstract—The Human Pregnane X Receptor (hPXR) is a nuclear receptor that regulates the expression of phase I and phase II drug-metabolizing enzymes, as well as that of drug transporters. Because this receptor plays a critical role in protecting tissues from potentially toxic endo- and xenobiotics, highly active agonists could represent novel therapeutic tools in treating several human diseases. Using an in vitro screening reporter system that allow to characterize hPXR activators and a first step of chemical modifications of an original agonist ligand (**C2BA-4**, 1-(2-chlorophenyl)-*N*-[1-(1-phenylethyl)-1*H*-benzimidazol-5-yl]methanesulfonamide), we identified compounds with a *N*-1*H*-benzimidazol-5-ylbenzenesulfonamide scaffold as a potent family of hPXR agonists. Further chemical modifications allowed us to identify enhanced activators, notably *N*-(1-benzyl-1*H*-benzimidazol-5-yl)-2,3,4,5,6-pentamethylbenzenesulfonamide (**6n**) with an EC_{50} value in the subnanomolar range. Accordingly to their potent EC_{50}, these compounds induced an efficient protection of hPXR against proteolytic digestion by trypsin even at very low ligand concentrations and were able to induce the expression of the main target genes of hPXR, *CYP3A4* and *CYP2B6*, in primary cultures of human hepatocytes.

1. Introduction

The Human Pregnane X Receptor (hPXR; NR1I2[1]), also known as SXR[2] and PAR,[3] is a member of the nuclear receptor (NR) superfamily which includes receptors for steroid and thyroid hormones as well as retinoids, cholesterol metabolites, and vitamins. hPXR is a ligand-dependent transcription factor which, upon heterodimerization with the retinoid X receptor (RXR),[2,4,5] interacts with a variety of DNA response elements (direct repeats DR-3, DR-4, and DR-5, and everted repeats ER-6 and ER-8) in the 5′-flanking regions of target genes. hPXR regulates the expression of cytochrome P450s, conjugating enzymes and ABC transporters involved in detoxification of human organism.[6] In particular, hPXR is the master regulator of the expression of CYP3A4 isoform, which metabolizes more than 60% of human drugs.[7] Thus, this nuclear receptor, which is activated by a large number of prescription drugs, is regarded as a xenobiotic sensor but is also at the origin of several clinically important drug–drug interactions.[6,8]

Even though hPXR was identified as a 'xenobiotic receptor', it also regulates the metabolism and availability of important endogenous compounds.[9–11] Indeed, steroid hormones and neuro-active steroids activate hPXR,[12] suggesting that this receptor plays a major role in many biological processes in diverse tissues. Recent studies indicated that hPXR plays a role in bilirubin clearance, prevents hyperbilirubinemia, and hepatorenal toxicity from cholesterol metabolites.[13] Also, when cholesterol metabolism is perturbed or toxic bile acids accumulate, hPXR switches on feedback and feed forward mechanisms to block bile acid production from cholesterol and to induce bile acid and oxysterol metabolic and transport pathways.[6,14] Activation of hPXR also inhibits the fibrosis response of the liver to chronic damage and the antifibrogenic mode of action is mediated

Keywords: Nuclear receptor; hPXR; Docking; Drug design.
* Corresponding author. Tel.: +33 4 67 54 86 44; fax: +33 4 67 52 96 23; e-mail: alain.chavanieu@cbs.cnrs.fr

0968-0896/$ - see front matter © 2008 Elsevier Ltd. All rights reserved.
doi:10.1016/j.bmc.2008.02.020

through changes in the expression of genes in hepatic stellate cells and liver macrophages.[15] Finally, hPXR is involved in lipid homeostasis by activating genes that facilitate lipogenesis and by suppressing the β-oxidative pathways.[16] The implication of hPXR in these metabolic pathways suggests that hPXR activators could have therapeutic applications for the treatment of several human diseases and might represent novel therapeutic tools.[10] Several agonists of hPXR with various chemical structures have been described including the cholesterol-lowering drugs lovastatin, the hypocholesterolemic drug SR12813.[1,17] Nevertheless original families of agonists with a high affinity remained to be identified.

Combining a structure-based and high-throughput virtual screening method with a functional approach using both cell- and whole animal-based assays, we recently proposed a strategy to identify highly active hPXR agonists.[18] Thus, we reported the identification of 13 new hPXR ligands and notably identified one agonist ligand named **C2BA-4** (**1**) with an EC_{50} of 49 ± 15 nM (Fig. 1) (1-(2-chlorophenyl)-*N*-[1-(1-phenylethyl)-1*H*-benzimidazol-5-yl]methanesulfonamide).

Here, based on this initial hit, we report the chemical optimization study of this initial hit which led to the identification of a series of agonist ligands that exhibit potent in vitro hPXR agonist activities and excellent efficacy in regulating CYP450 expression in human primary hepatocytes. In particular, we identified compound **6n** as a potent agonist of hPXR with active concentration in the subnanomolar range.

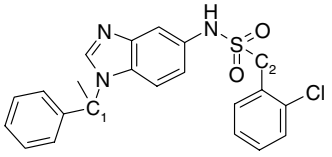

Figure 1. Structure of C2BA-4 (**1**), a previous hit.

2. Chemistry

To determine the structure–activity relationship of **C2BA-4** (**1**), several sulfonamide analogues were synthesized. 1-Benzyl-1*H*-benzimidazol-5-amine moiety found in several compounds was synthesized according to Scheme 1. 5-Nitrobenzimidazole was alkylated with benzyl bromide in the presence of potassium carbonate in butanone[19] to give a mixture of 1-benzyl-5-nitro-1*H*-benzimidazole **2** and its N3 regioisomer **3**. The nitro group was then reduced by treatment with $SnCl_2$ in dry EtOH to afford the required compound 1-benzyl-1*H*-benzimidazol-5-amine **4** and its N3 regioisomer **5**. Compounds **4** and **5** were separated by chromatography and the desired regioisomer **4** (yield 34%) was identified through ^{1}H NMR experiments (NOE). The sulfonamide analogues **6a**–**p** and **7a**–**b** were obtained by the condensation of compounds **4** or **5** with commercial sulfonyl chlorides or 2-chlorophenylmethanesulfonyl chloride in dry THF and in the presence of NEt_3 (Schemes 2 and 3) in good yields. To obtain the 1-benzyl-1*H*-indol-5-amine moiety of compound **8**, the 5-nitroindole was alkylated with benzyl bromide,[19] then the nitro group was reduced. Compound **8** was then obtained by the condensation of the 1-benzyl-1*H*-indol-5-amine moiety with 2-chlorophenylmethanesulfonyl chloride (Scheme 4, yield 80%). The urea analogues, compounds **9a**–**c**, were prepared by the condensation of compound **4** with aryl isocyanates (Scheme 5) in good to excellent yields. The synthesis of amide derivatives, compounds **10a**–**c** (Scheme 6) proceeded by the condensation of compound **4** with carboxylic acids in CH_2Cl_2 and in the presence of TBTU,[20] DIEA to afford amide derivatives **10a**–**c** in good yields. The 1-hexyl-1*H*-benzimidazol-5-amine moiety found in compounds **14a**–**b** and the 1-(naphthalen-2-ylmethyl)-1*H*-benzimidazol-5-amine group found in compounds **15a**–**b** were synthesized according to the Scheme 7. 5-Nitrobenzimidazole was alkylated with 1-bromohexane or with 2-(1-bromomethyl) naphthalene to give a mixture of two regioisomer derivatives (compounds **11a**–**b** and **12a**–**b**, respectively). In the case of compounds

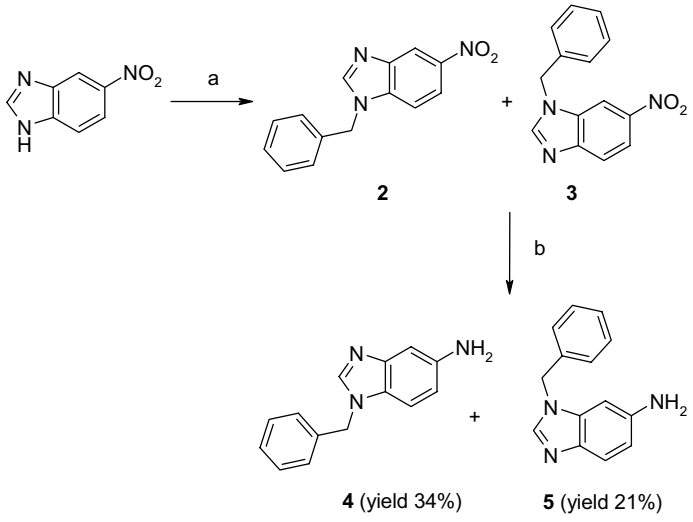

Scheme 1. Reagents and conditions: (a) BnBr, K_2Co_3, butanone, reflux; (b) $SnCl_2$, EtOH, reflux.

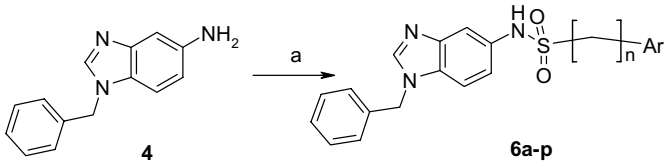

6a : n=1, Ar=2-chlorophenyl (yield 31%)
6b : n=1, Ar=2-nitrophenyl (yield 76%)
6c : n=0, Ar=2-chlorophenyl (yield 40%)
6d : n=0, Ar=2-bromophenyl (yield 42%)
6e : n=0, Ar=2-fluorophenyl (yield 42.5%)
6f : n=0, Ar=2-nitrophenyl (yield 13%)
6g : n=0, Ar=4-nitrophenyl (yield 18%)
6h : n=0, Ar=1-naphthyl (yield 39%)
6i : n=0, Ar=2-naphthyl (yield 44%)
6j : n=0, Ar=4-biphenyl (yield 69%)
6k : n=0, Ar=2-methylphenyl (yield 18%)
6l : n=0, Ar=3,5-dimethylphenyl (yield 18%)
6m : n=0, Ar=2,4,6-trimethylphenyl (yield 46%)
6n : n=0, Ar=pentamethylphenyl (yield 66%)
6o : n=0, Ar=4-tertbutylphenyl (yield 36%)
6p : n=0, Ar=4-propylphenyl (yield 76%)

Scheme 2. Reagents and condition: (a) Ar-$(CH_2)_n$–SO_2Cl, NEt_3, THF, reflux.

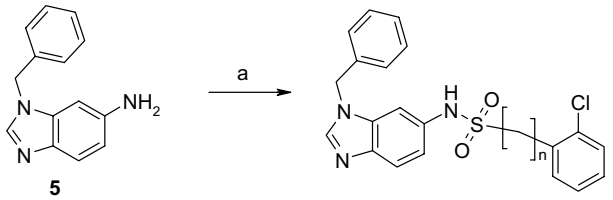

7a : n=1 (yield 46%)
7b : n=0 (yield 12%)

Scheme 3. Reagents and condition: (a) Ar-$(CH_2)n$–SO_2Cl, NEt_3, THF, reflux.

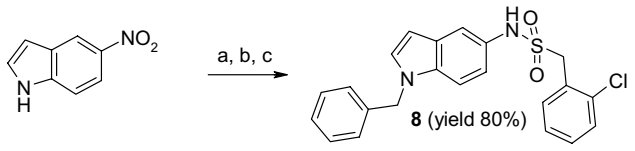

Scheme 4. Reagents and conditions: (a) BnBr, K_2CO_3, butanone, reflux; (b) $SnCl_2$, EtOH, reflux; (c) 2-chlorophenylmethanesulfonyl chloride, NEt_3, THF, reflux.

11a–**b** the desired N1 regioisomer **11a** (yield 54%) was separated by chromatography on silica gel and identified through ^{1}H NMR experiment, before the reduction of the nitro group. Whereas for compounds **12a**–**b**, due to a difficulty to separate compounds at this step, the purification was performed after the reduction. The nitro group was reduced to give the required compounds, 1-hexyl-1*H*-benzimidazol-5-amine (**13a**, yield 41%) and 1-(naphthalen-2-ylmethyl)-1*H*-benzimidazol-5-amine (**13b**, yield 32%). Then, compounds **14a**–**b** and **15a**–**b** were obtained by the condensation with 2-chlorobenzenesulfonyl chloride or pentamethylbenzenesulfonyl chloride in dry THF and in the presence of NEt_3 in good yields.

3. Results and discussion

3.1. New lead selection and synthesis of derivatives

hPXR agonist activities as well as hPXR-independent luciferase expression were evaluated as already de-

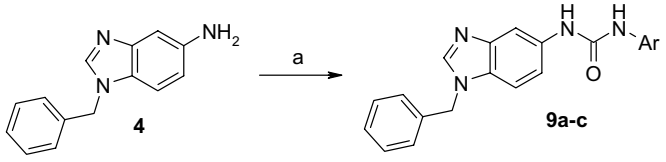

9a : Ar=2-chlorophenyl (yield 87%)
9b : Ar=2-nitrophenyl (yield 63%)
9c : Ar=1-naphthyl (yield 56%)

Scheme 5. Reagents and condition: (a) aryl isocyanate, THF, reflux.

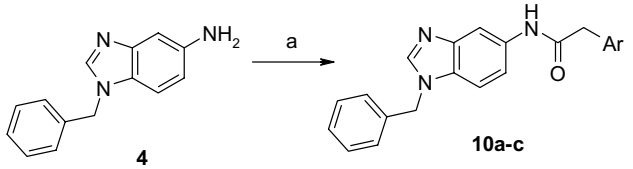

10a : Ar=2-chlorophenyl (yield 71%)
10b : Ar=1-naphthyl (yield 63%)
10c : Ar=2-naphthyl (yield 21%)

Scheme 6. Reagents: (a) Ar-CH_2COOH, TBTU, DIEA, CH_2Cl_2.

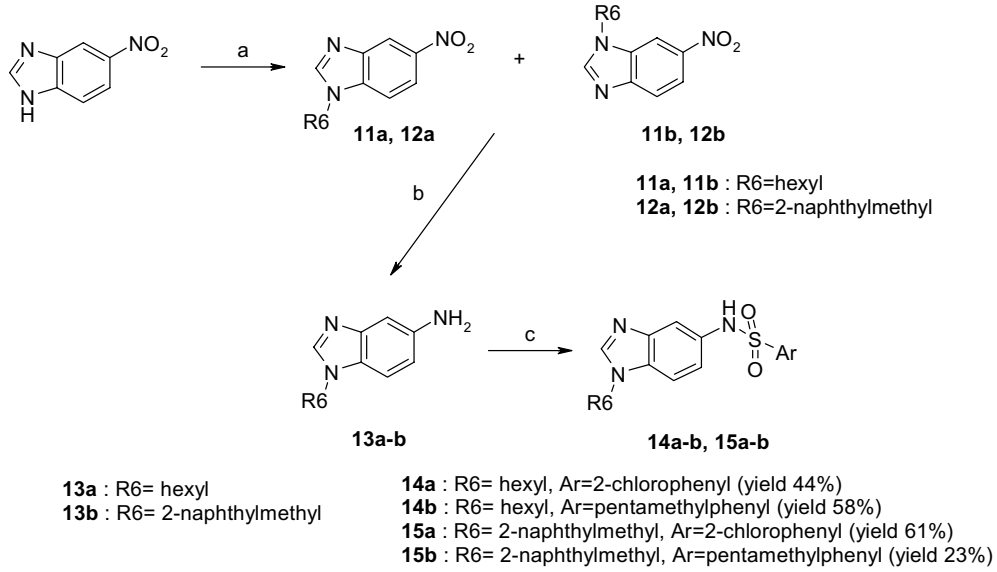

Scheme 7. Reagents (a) R-CH_2Br, K_2CO_3, butanone, reflux; (b) $SnCl_2$, EtOH, reflux; (c) Ar-SO_2Cl, NEt_3, THF, reflux.

scribed.[21,18] Briefly, to detect hPXR agonists, HGPXR cell line[22] that stably express hPXR was used and the activation values obtained with all the tested compounds were expressed relative to the luciferase activity observed in the presence of 1 μM of the human and rabbit PXR activator[17] SR12813 (taken as 100%). To assess the hPXR-independent luciferase expression as well as the toxicity, all compounds were systematically tested for their ability to activate parent HG_5LN cells.[22,18]

Based on **C2BA-4** (**1**), an initial attempt to identify a new lead compound consisted in removing the CH_3 group responsible for the chirality, and the methylene group (position C1 and C2, respectively, Fig. 1). **C2BA-4** used as a racemic solution showed an EC_{50} of 49 nM (Table 1 and supporting information) and removing the CH_3 group (**6a**, EC_{50} = 176 nM) increased the EC_{50} value by a factor of 3.5. Compound **6c** without the CH_3 group responsible for the chirality and without the methylene group presented a twofold decrease of the EC_{50} value (EC_{50} = 23 nM) which indicated that the methylene group has a deleterious effect on the agonist activity. We also investigated the effect of the replacement of the chloride atom on **C2BA-4** by a 2-nitro moiety and found an attenuated agonist activity (**6b**, EC_{50} = 428 nM). The synthesis of **6a** and **6c** provided an intermediary by-product (**5**), a regioisomer of compound **4** with a benzyl group at the N3-position on the benzimidazole ring (Scheme 1). Compound **5** led to **7a** and **7b** which both showed a lower potency (EC_{50} of 376 nM and 340 nM, respectively) than **C2BA-4** and a high cellular toxicity at 10 μM (data not shown). In order to investigate the influence on the agonist activity of an indole moiety, compound **8** was synthesized. This compound was as potent as **6a** with an EC_{50} of 197 nM but exhibited a higher cellular toxicity at 10 μM (data not shown).

Then, to precise the importance of the sulfonamide moiety, the central part of the molecule **C2BA-4** was replaced with an urea (Table 2) which led to a much less

Table 1. Data of EC_{50} values obtained on HGPXR reporter cell lines of compounds **C2BA-4**, **6a**–**c** and **7a**–**b**

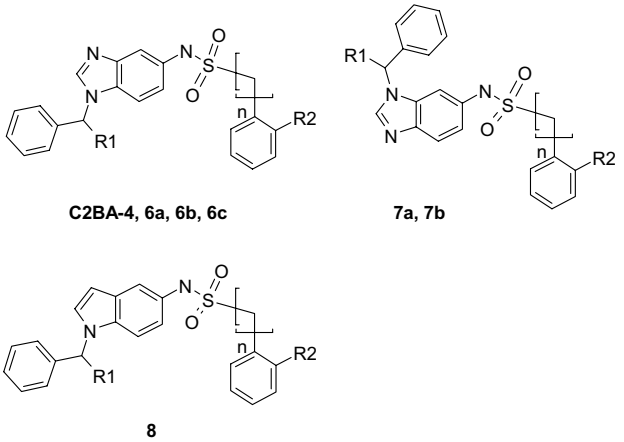

Compound	*n*	R1	R2	EC_{50}[a] (nM) (*n*)
C2BA-4 (**1**)	1	Me	Cl	49 ± 15 (3)
6a	1	H	Cl	176 ± 73 (3)
6b	1	H	NO_2	428 ± 104 (3)
6c	0	H	Cl	23 ± 10 (4)
7a	1	H	Cl	376 ± 230 (2)
7b	0	H	Cl	340 ± 110 (2)
8	1	H	Cl	197 ± 200 (2)

C2BA-4 is used as a racemic solution. EC_{50}, concentration of molecule required for 50% hPXR activation, data represent mean values ± SD.
[a] Number of independent experiments in triplicate.

potent compound (**9a**, EC_{50} = 1476 nM). This decrease being even more marked if the chlorophenyl moiety was replaced with a 2-nitro-phenyl (**9b**) or a 1-naphthyl group (**9c**) (EC_{50} > 5000 nM). The substitution of the sulfonamide moiety by an amide (**10a**) also induced a decrease of the agonist activity (EC_{50} = 515 nM) and a 1-naphthyl instead of the chlorophenyl moiety slightly restored the agonist activity (**10b**, EC_{50} = 217 nM). By contrast a 2-naphthyl was not favorable (**10c**,

Table 2. Data of EC_{50} values obtained on HGPXR reporter cell lines of compounds **9a–c** and **10a–c**

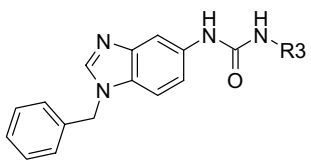

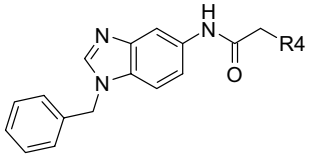

Compound	R3	EC_{50} ± SD[a] (nM) (*n*)	Compound	R4	EC_{50} ± SD[a] (nM) (*n*)
9a	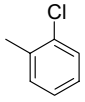	1456 ± 746 (3)	**10a**	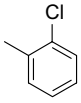	515 ± 281 (3)
9b	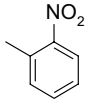	>5000 (2)	**10b**	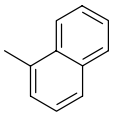	217 ± 144 (3)
9c	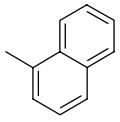	>5000 (2)	**10c**	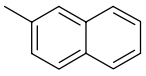	>5000 (2)

EC_{50}, concentration of molecule required for 50% hPXR activation, data represent mean values ± SD.
[a] Number of independent experiments in triplicate.

EC_{50} > 5000 nM). Tested in competition in presence of SR12813 (0.3 μM), compounds **9b**, **9c**, and **10c** at 10 μM and 1 μM were not found to present an antagonist activity (data not shown).

Consequently, the most active compound **6c** with a sulfonamide group, no element of chirality at position C1 and no methylene group at position C2, was selected as the new lead compound and served as the standard for further potency comparison.

We turned our attention to the nature of the substituent on the phenyl ring and a series of **6c** derivatives were synthesized (Table 3). At first, the 2-chloride atom on the phenyl group was substituted by electron-withdrawing groups. Despite the higher steric hindrance, replacement by a bromide atom led to the same potency (**6d**, EC_{50} = 20 nM), whereas the *o*-substitution of the phenyl ring with the small electron-withdrawing fluorine atom (**6e**, EC_{50} = 101 nM) and the larger electron-withdrawing nitro moiety (**6f**, EC_{50} = 271 nM), resulted in a significant loss of activity. A 15-decrease of the agonist activity was observed with a nitro group on the para position of the phenyl ring (**6g**, EC_{50} = 336 nM). We then investigated the effect of the replacement of the phenyl ring by larger aromatic moieties and found that a 2-naphthyl and preferentially a 1-naphthyl led to potent compounds whereas a biphenyl group was not favorable (**6i**, EC_{50} = 51 nM, **6h**, EC_{50} = 20 nM, **6j**, EC_{50} = 388 nM, respectively). Then, 2-methyl and 3,5-dimethyl phenyl derivatives were synthesized and led to a slight decrease of the agonist activity (**6k**, EC_{50} = 45 nM, **6l**, EC_{50} = 33 nM) when compared to **6c** whereas a sharp increase in potency was observed through introduction of three (**6m**) and five (**6n**) methyl groups on the phenyl ring as the EC_{50} was 1.5 nM and 0.7 nM, respectively. In contrast, bulkier substituents such as *tert*-butyl or propyl groups in *para*-position (**6o**, EC_{50} = 42 nM, **6p**, EC_{50} = 52 nM) led to potent but less active compounds when compared with compound **6c** or the highest active compound **6n**. These results thus indicated that the phenyl group of **6c** can be substituted with various—preferentially small—aliphatic or aromatic moieties whereas bulkier lipophilic groups are less tolerated.

In a next step, we investigated the influence of the benzyl group in the activity potency of our analogues (Table 4). Compounds **14a** with a hexyl moiety in replacement of the benzyl group presented a twofold decreased activity (EC_{50} = 55 nM) when compared to compound **6c** and a 2-naphthylmethyl increased the EC_{50} value to 385 nM (**15a**). The replacement of the 2-chlorophenyl group by a pentamethylphenyl restored the activity and led to relatively potent compounds (**14b**, EC_{50} = 13 nM, **15b**, EC_{50} = 55 nM).

3.2. Docking studies and binding mode analysis of compound 6n

Crystal structures of the ligand-binding domain (LBD) of hPXR have been obtained in its apo conformation, as well as in complex with the endogenous ligand 17β-estradiol[23] or xenobiotic compounds (rifampicin,[24] SR12813,[25] hyperforin,[26] and T0901317[27]) and with fragments of the human transcriptional co-activator SRC-1. These studies revealed a large, with 20 hydrophobic amino acids and eight polar residues capable of forming hydrogen bonds, and conformable binding pocket that contributes to the ability of hPXR to respond to compound of varying size and shape through

Table 3. Data of EC_{50} values obtained on HGPXR reporter cell lines of compounds **6d–p**

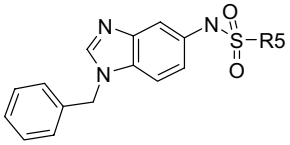

Compound	R5	EC_{50} ± SD[a] (nM) (*n*)	Compound	R5	EC_{50} ± SD[a] (nM) (*n*)
6d		20 ± 8	**6k**		45 ± 13
6e		101 ± 33	**6l**	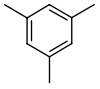	33 ± .11
6f		271 ± 98	**6m**		1.5 ± 0.5
6g	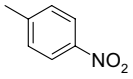	336 ± 217	**6n**	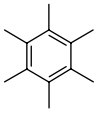	0.7 ± 0.3
6h	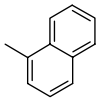	20 ± 9	**6o**	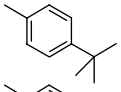	42 ± 10
6i	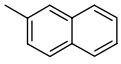	51 ± 16	**6p**	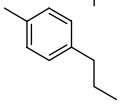	52 ± 12
6j	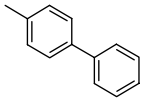	388 ± 105			

EC_{50}, concentration of molecule required for 50% hPXR activation, data represent mean values ± SD.
[a] Number of independent experiments in triplicate.

a combination of hydrophobic and polar interactions. Unlike other nuclear receptors, hPXR LBD displays a 60 residue insertion (sequence 175–235) which generates an extended five-stranded antiparallel β-sheet, instead of the canonical three-stranded antiparallel β-sheet,[28] and participates to the α2 helical region (sequence 192–209) that change its position and its secondary structure to accommodate different types of ligands.[27,24–26,29]

The binding mode of compound **6n** into the LBD of hPXR was analyzed by the program Surflex-2.1[30,31] and by using the recently reported 2.8 Å resolution structure of hPXR in complex with compound **T0901317** (**T1317**) and a 88-amino acid fragment of human SRC-1[27] (code pdb: 2O9I). In this structure, **T1317** interacts via Van der Waals contacts with hydrophobic residues constantly involved in ligand binding such as Met 243, Trp 299, and Phe 420 as well as, for polar contacts, with Gln 285 and His 407 but also with never previously described residues such as Tyr 306 and His 327.

When performed in the absence of restraint, our docking studies revealed a putative binding mode for **6n** in which the pentamethylphenyl group lies at interacting distance of the hydrophobic side chain of Trp 299 and Y306 (3.5 Å), whereas the benzyl moiety could interact with Leu 206, Leu 240, Leu 411, Phe 420, and Met 425 (from 2.5 Å to 4.5 Å) (Fig. 2A). Intriguingly, no significant polar contribution to docking scores was observed despite the presence of several hydrophilic residues in the ligand-binding pocket (Ser 247, Gln 285, His 327, and His 427) and the sulfonamide moiety of compound **6n**.

Additional docking studies were performed using Surflex through an implemented method that relies on a placed molecular fragment. Interestingly, the sulfonamide derivative **6n** shows a common *N*-phenyl-benzenesulfonamide group with the agonist **T1317** (Fig. 2B) which presented an EC_{50} about 9.8 nM in our transactivation test (see supplementary data) in perfect agreement with the value reported by Xue et al.[27] Indeed, the *N*-phenyl-benzenesulfonamide group of **T1317** can be used as an anchoring point during the Surflex docking process. When docking was carried out under this condition (see supplementary data), **6n** presents a similar orientation in the hPXR LBP as described above (Fig. 2A–C) with the pentamethylphenyl group directed toward the β-sheet region of hPXR and at interacting distances with three hydrophobic side chain residues Phe 288, Trp 299, and Tyr 306 (3.5 Å). This

Table 4. Data of EC_{50} values obtained on HGPXR reporter cell lines of compounds **14a–b** and **18a–b**

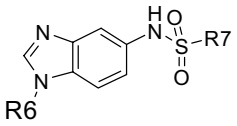

Compound	R7	R7	EC_{50} ± SD[a] (nM) (*n*)
14a	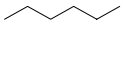		55 ± 32 (4)
14b	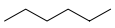	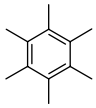	13 ± 5 (4)
15a	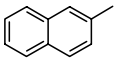		385 ± 239 (4)
15b	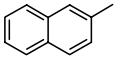	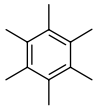	55 ± 19 (3)

EC_{50}, concentration of molecule required for 50% hPXR activation, data represent mean values ± SD.
[a] Number of independent experiments in triplicate.

putative mode of binding is in good agreement with activity results obtained with compounds **6d–p**, which underlined that aliphatic or aromatic substituents on the phenyl ring led to highly active compounds. Then, according to fragment restraint, the *N*-1*H*-benzimidazol-5-ylbenzenesulfonamide group is found close to the place occupied by the *N*-phenyl-benzenesulfonamide group of **T1317** (see supplementary data) and could form two putative hydrogen bonds in the central part of the cavity, one with His 307 and one with Gln 285 (<3 Å). In this docking condition, the benzyl group of **6n** was found close to the residue Phe 420 (<3 Å) from Helix-12 which is part of the AF-2 surface implied in the recruitment of co-activators,[24–26,29,27,23] as well as close to the side chain of residues Leu 240 (<3 Å) and Ile 414 (<4 Å). The benzyl group of **6n** was also found at interacting distance (<3 Å) of Leu 206, a residue of the mobile α2 region that contributes to hPXR ligand accommodation. Interestingly, this putative mode of binding could explain the potent agonist activity of several compounds bearing, instead of the benzyl group, a bulkier hexyl (**14a–b**) or 2-naphthylmethyl (**15a–b**) moieties, which then are directed toward this mobile region upon the binding to hPXR.

This hypothesis is in agreement with a previous report of Xue et al.,[27] which demonstrated that several analogues of **T1317** bearing bulky substituent, with the goal of ste-

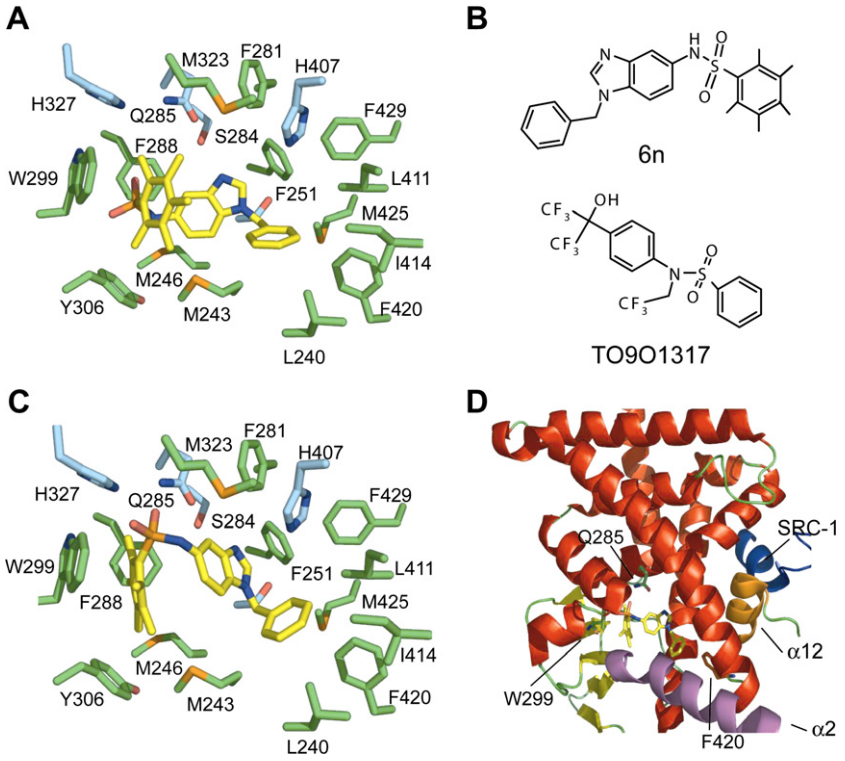

Figure 2. Putative binding mode of compound **6n** within the ligand pocket of the LBD of hPXR. (A) Compound **6n** docked with no restraint presents the pentamethylphenyl group directed toward Trp 299 and Tyr 306 and the benzyl moiety close to Phe 420 and Met 425 but no polar contribution to binding of the sulfonamide central part. Residues forming hydrophobic interactions are in green while those forming polar contacts are rendered in blue. (B) Chemical structures of **6n** and **T0901317**. (C) Compound **6n** docked under fragment restraint using the *N*-phenyl-benzenesulfonamide part of **T0901317** (code pdb: 2O9I). To clarify, Leu 206 and Leu 209 were not represented. (D) Compound **6n** docked with constraint within the human PXR LBD/SRC-1 complex (monomer, 2O9I) with α-helices rendered in red except: helix 12 in orange, the mobile α2 region is purple and the SRC1 fragment in blue. β-Sheets are in yellow and the carbon atoms of compound **6n** in yellow. The side chains of residues W299, Q285, and F420 are represented in sticks.

rically disrupting αAF position, led to effective agonists rather than antagonists. Thus, crystal structures of the hPXR LBD in complex with various ligands have revealed that part of the α2 region is structurally variable, from α helix to completely disordered, and participates to the ligand-binding pocket accommodation to large ligand such as rifampicin,[24] **T1317** analogues.

3.3. Limited proteolytic digestion

In a previous study,[18] **C2BA-4** was reported to interact with the LBD of hPXR. Here, to confirm whether the most highly active compounds **6c**, **6m**, and **6n** could directly bind and induce conformational changes in hPXR, we analyzed its resistance to limited proteolysis (Fig. 3 and supporting information). LBD of hPXR labeled with [^{35}S]methionine was pre-incubated with ethanol (vehicle) or increasing concentrations (0.3–10 μM) of compounds **C2BA-4**, **6c**, **6m**, and **6n**, then digested with 250 μg/ml trypsin. Incubation of the receptor with 250 μg/ml trypsin in the absence of ligand (ETOH) led to complete digestion of hPXR-LBD. In contrast, all the four ligands produced a 30 kDa major protease resistant fragment. These results indicate that compounds **6c**, **6m**, and **6n** interact directly with hPXR LBD. In agreement with the activities of these four ligands on HGPXR cell line, compounds **6m** and **6n**, which exhibited the best agonist activities, protected hPXR up to very low concentrations (EC_{50} = 8 nM). **C2BA-4** and compound **6c** were less potent on hPXR, and the receptor protection only occurred at higher concentrations (EC_{50} = 0.81 μM and 0.16 μM, respectively).

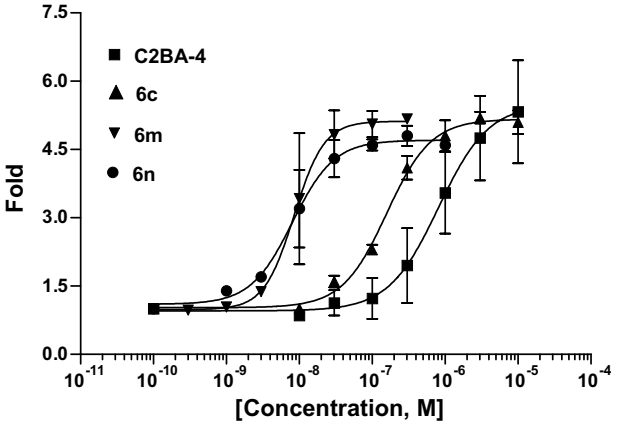

Figure 3. Binding of **C2BA-4** and compounds **6c**, **6m**, and **6n** to hPXR. hPXR protein was synthesized and labeled with [35S]methionine in reticulocyte lysate and incubated with the four ligands or vehicle alone before trypsin digestion. The reaction was terminated by boiling in SDS-containing protein sample buffer. hPXR proteolytic pattern was analyzed by SDS–PAGE and fixed/dried gel was visualized by PhosphorImager (see supplementary data). This figure is representative of three experiments. Autoradiograms were analyzed using an image analyzing software. To measure the relative levels of the 30 kDa band protected by the four ligands on SDS–PAGE gel, the intensity of the band of hPXR-LBD treated with ethanol was taken as 1. The axis labeled protection shows the ratio (level of the 30 kDa band incubated with ligand/ level of the band treated with ethanol). **C2BA-4**: EC_{50} = 809 ± 150 nM, **6c**: EC_{50} = 157 ± 44 nM, **6m**: EC_{50} = 8.05 ± 0.45 nM, **6n**: EC_{50} = 8.04 ± 1.9 nM.

3.4. 6c, 6m, and 6n induce CYP3A4 and CYP2B6 mRNA expression in cultured human hepatocytes

To further characterize **6c**, **6m**, and **6n** as potent human PXR ligands, we studied their effects on *CYP3A4* and *CYP2B6* genes transcription[4,13] in primary culture of human hepatocytes. Hepatocytes from 4 different donors were treated with the solvent control (DMSO 0.1%), SR12813 (1 μM), **6c** (1 μM), **6m** (1 μM), and **6n** (1 μM) for 24 h. Total mRNA was isolated and real-time PCR analysis was performed to detect the expression level of GAPDH, β-actin, CYP3A4, and CYP2B6 mRNAs. We evaluated the induction ratios (mRNA levels in treated cells compared with control cells after normalization with respect to GAPDH signal). β-Actin mRNA levels were used as quality controls of RNA preparations and RT reactions. As expected, SR12813 strongly increased CYP3A4 and CYP2B6 mRNA expressions in these cells (Table 5 and Fig. 4), while β-actin RNA level was unchanged whatever the compound tested. Interestingly, **6c**, **6m**, and **6n** molecules significantly increased CYP3A4 and CYP2B6 mRNAs levels in all culture preparations. Moreover, **6n**, which is the most active compound (EC_{50} = 0.7 nM) in our HGPXR cell line, induced the expression level of CYP3A4 and CYP2B6 mRNAs stronger than SR12813 at the same concentration in the three culture preparations tested (Table 5). In addition, we observed in two different primary cultures (FT271 and FT272) that the increases of CYP3A4 and CYP2B6 mRNAs levels by **6c**, **6m**, and **6n** were dose dependent (Fig. 4), with **6c** showing the most pronounced effect at the lowest concentration tested (0.1 μM). These results demonstrated that, in agreement with our in vitro studies, **6c**, **6m**, and **6n** are able to activate hPXR in human hepatocytes, leading to an increase of transcription of its main target genes such as *CYP3A4* and *CYP2B6*. Even if the response levels were different between donors, it is important to note that CYP3A4 and CYP2B6 are inducible enzymes and their induction varies markedly (up to 40-fold) across the population due to drug-mediated variation in CYP transcription.[32,12]

4. Conclusion

In conclusion, hPXR has emerged as a potential therapeutic target in several human diseases. This nuclear receptor presents the particularity to bind a large variety of endogen metabolites and xenobiotics usually with a micromolar affinity. Only few compounds with a submicromolar activity have been described so far (SR12813, T0901317, Hyperforin). Among them, we recently reported an original compound **C2BA-4** which was suitable for chemical optimizations.

In this report, we first identified a *N*-1*H*-benzimidazol-5-ylbenzenesulfonamide scaffold that allow the design of potent hPXR agonist ligands. Then, as judged on a reporter cell line system and by limited proteolytic digestion, as well as on the expression of CYP3A4 and CYP2B6 by human hepatocytes in culture, various chemical modifications allowed us to identify a potent li-

Table 5. Effects of compounds **6c**, **6m**, and **6n** on the expression of hPXR target genes in cultured human hepatocytes

	Donor #1 (FT 268)		Donor #2 (FT 269)		Donor #3 (FT271)		Donor #3 (FT272)	
	CYP3A4	**CYP2B6**	**CYP3A4**	**CYP2B6**	**CYP3A4**	**CYP2B6**	**CYP3A4**	**CYP2B6**
SR12813	4.02 ± 0.66	3.26 ± 0.23	10.90 ± 0.79	3.74 ± 0.56	11.84 ± 1.03	2.00 ± 0.34	24.01 ± 0.88	3.91 ± 0.18
6c	7.23 ± 0.74	3.02 ± 0.31	17.04 ± 1.93	10.46 ± 1.38	9.97 ± 0.92	3.05 ± 0.46	36.06 ± 2.34	11.83 ± 0.77
6m	ND	ND	ND	ND	15.58 ± 1.10	1.89 ± 0.36	31.68 ± 2.58	7.55 ± 0.50
6n	ND	ND	29.02 ± 4.5	14.89 ± 2.19	14.91 ± 3.07	4.86 ± 1.07	32.59 ± 0.65	11.41 ± 1.15

Human hepatocytes from four different donors (FT268, FT269, FT271, and FT272) were treated for 24 h with solvent (DMSO 0.1%), SR12813 (1 μM), compounds **6c**, **6m**, and **6n** (1 μM). Twenty hours later, cells were harvested in TRIzol, total RNA was extracted and cDNA was synthesized from 1 μg of total RNA using Superscript II. CYP3A4 and CYP2B6 mRNA levels were measured via quantitative real-time PCR using the Light Cycler apparatus. As an internal control, the β-actin mRNA level was measured similarly to normalize data. Induction ratios (mRNA in inducer-treated cells/mRNA in untreated cells) ± standard errors are presented here. ND: non-determined.

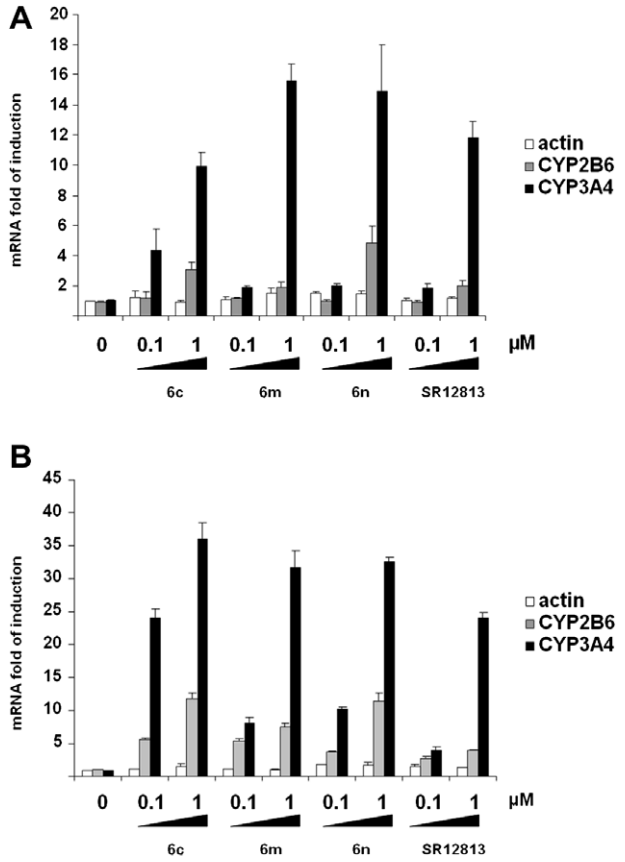

Figure 4. Effect of **SR12813**, **6c**, **6m**, and **6n** on CYP3A4 and CYP2B6 mRNA expression in human hepatocytes. Human hepatocytes (FT2171 (A) and FT272 (B)) were cultured in presence of SR12813, **6c**, **6m**, and **6n** molecules at 0.1 μM or 1 μM for 24 h. CYP3A4, CYP2B6, β-actin (actin), and GAPDH mRNAs were quantified by real-time RT-PCR analysis. Values were normalized with respect to GAPDH mRNA level. Induction ratios (mRNA in inducer-treated cells/mRNA in untreated cells) ± standard errors are presented here.

gand with subnanomolar EC_{50}, which represents the most active compound described so far for hPXR. Therefore, *N*-1*H*-benzimidazol-5-ylbenzenesulfonamide derivatives represent an original family of potent agonists of hPXR that might serve as novel leads for further pharmacological investigations as therapeutic agonist agents against human metabolic or neurodegenerative diseases.[10,33]

5. Experimental

5.1. General methods

All reagents and solvents were purchased from commercial sources and used without further purification. Melting points were determined on a Kofler block and are uncorrected. Mass spectra were acquired under fast atom bombardment (FAB) conditions using a Jeol JMS DX300, and samples were introduced on a matrix. Proton NMR spectra were collected on a Bruker 400 MHz spectrometer using tetramethylsilane (TMS) as internal standard, and chemical shift (δ) data are reported in parts per million (ppm) relative to internal standard TMS. Separations by chromatography on silica column were carried out by using silica gel SDS 60 (mesh 35–70) with hexane, ethyl acetate (AcOEt), cyclohexane, and methanol (MeOH) as eluents with chromatographic solvents expressed in volume/volume basis. The reported chemical yields were not optimized. Materials for cell culture, RNA extraction TRIzol reagent, SuperScript-II First-Strand Synthesis System for RT-PCR, and Lipofectamine were from Invitrogen (Cergy-Pontoise, France). Luciferin and G418 were purchased from Promega (Charbonnières-les-Bains, France). SR12813 was purchased from Tebu-bio (Le Perray en Yvelines, France).

5.1.1. Synthesis of 1-benzyl-5-nitro-1*H*-benzimidazole (2) and 3-benzyl-5-nitro-3*H*-benzimidazole (3). 5-Nitrobenzimidazole (30.65 mmol) and benzyl bromide (33.68 mmol) was dissolved in 155 ml of butanone. Potassium carbonate was then added (33.68 mmol). The reaction mixture was stirred under reflux for 3 h then concentrated under reduced pressure and dissolved in ethyl acetate. Formed salts were filtrated and the filtrate was concentrated again. The solid obtained was washed with cyclohexane (100 ml), and then dried under vacuum to give a mixture (orange red solid, 30.63 mmol, 99%) of the required 1-benzyl-5-nitro-1*H*-benzimidazole (**2**) and its N3 regioisomer (**3**).

5.1.2. Synthesis of 1-benzyl-1*H*-benzimidazol-5-amine (4) and 3-benzyl-3*H*-benzimidazol-5-amine (5). The mixture containing compounds **2** and **3** (15.81 mmol) was dissolved in 165 ml of absolute ethanol and $SnCl_2$ dihydrate (82.45 mmol) was then added. The reaction mixture was stirred under reflux for 3 h then concentrated under reduced pressure and dissolved in 165 ml of ethyl acetate. Sodium bicarbonate (200 ml) was then added. Formed

salts were filtrated and washed with 50 ml of AcOEt. The organic phase of the filtrate was washed with water (100 ml), dried on anhydrous sodium sulfate, filtrated, and concentrated under reduced pressure to give a mixture of compound **4** and its N3 regioisomer **5**. Then, this mixture was purified by chromatography on silica gel (AcOEt/MeOH 9:1). Two fractions were obtained, one contained the N3 regioisomer **5** (3.45 mmol 21%, $R_f = 0.48$), the other contained the required **1-benzyl-1*H*-benzimidazol-5-amine 4** (5.43 mmol, 34%, $R_f = 0.24$). The two fractions were pink-orange color solids.

5.1.3. Synthesis of sodium 2-chlorobenzyl sulfonate. The 2-chlorobenzyl chloride (122.99 mmol) and sodium sulfite (124.17 mmol) were dissolved in water (100 ml). The reaction mixture was heated (100 °C) under reflux for 5 h then concentrated under reduced pressure. The white solid obtained was filtrated, washed with diethylic ether (100 ml) then dried under vacuum (120.99 mmol, 97%).

5.1.4. Synthesis of 2-chlorophenylmethanesulfonyl chloride. The sodium 2-chlorobenzyl sulfonate (43.76 mmol) was put in the presence of phosphorus oxychloride (219.0 mmol). The reaction mixture was heated (105 °C) under reflux for 6 h then filtrated (elimination of formed salts). Formed salts were washed with dichloromethane (50 ml). The filtrate was successively washed with water (1 * 20 ml), with a saturated solution of $NaHCO_3$ (2 * 20 ml) then with 0.25 N NaOH solution (1 * 20 ml). Then, the organic phase was dried on anhydrous sodium sulfate, filtrated then concentrated under reduced pressure to give a white solid (15.95 mmol, 36%).

5.1.5. Synthesis of sulfonamide analogues (6a–p, 7a–b, 14a–b, and 15a–b): general procedure (except for 8). The compound **4** or **5** or **13a** or **13b** (0.45 mmol) and triethylamine (0.45 mmol) were dissolved in dry THF (10 ml). The mixture was placed under agitation and sulfonyl chloride (0.45 mmol) was then added. The mixture was stirred under reflux for 20 h, concentrated under reduced pressure then dissolved in dichloromethane (10 ml). The organic phase was successively washed with a citric acid solution (1× 15 ml), with brine (1× 5 ml), with a saturated solution of $NaHCO_3$ (1× 15 ml) and finally with brine (1× 5 ml). Then, the organic phase was dried on anhydrous sodium sulfate, filtrated then evaporated. All the sulfonamide derivatives **6a**–**p**, **7a**–**b**, **14a**–**b**, and **15a**–**b** were purified by chromatography on silica gel.

5.1.6. Synthesis of *N*-(1-benzyl-1*H*-indol-5-yl)-1-(2-chlorophenyl)methanesulfonamide (8). 5-Nitroindole (30.83 mmol) and the benzyl bromide (33.91 mmol) were dissolved in 150 ml of butanone. Potassium carbonate (34.03 mmol) was then added. The reaction mixture was stirred under reflux for 23 h then concentrated under reduced pressure and dissolved in 150 ml of ethyl acetate. Formed salts were filtrated and the filtrate was concentrated under reduced pressure. The solid obtained was washed with 100 ml of cyclohexane then filtrated and dried under vacuum to give the 1-benzyl-5-nitro-1*H*-indole (29.45 mmol, 96%) a yellow solid. This product (11.89 mmol) was dissolved in 150 ml of absolute ethanol. The mixture was stirred under agitation and $SnCl_2$ (59.40 mmol) was then added. The reaction mixture was stirred under reflux for 18 h then concentrated under reduced pressure and dissolved in 150 ml of ethyl acetate. Sodium bicarbonate (200 ml) was then added. Formed salts were filtrated and washed with 500 ml of AcOEt. The organic phase of the filtrate was washed with brine (1× 100 ml), dried on anhydrous sodium sulfate, filtrated, and concentrated under reduced pressure. The solid was purified by chromatography on silica gel (hexane/AcOEt 6:4) to afford the 1-benzyl-1*H*-indol-5-amine as a red solid (10.84 mmol, 81%). The 1-benzyl-1*H*-indol-5-amine (0.45 mmol), and triethylamine (0.45 mmol) were dissolved in 10 ml of dry THF. The mixture was placed under agitation and the (2-chlorophenyl)-methanesulfonyl chloride (0.45 mmol, 1 equiv) was then added. The reaction mixture was stirred under reflux for 6 h, concentrated under reduced pressure, then dissolved in 20 ml of dichloromethane. The organic phase was washed with citric acid (2× 10 ml) and with brine (1× 10 ml). Then, the organic phase was dried on anhydrous sodium sulfate, filtrated then evaporated. The crude product was purified by chromatography on silica gel (hexane/AcOEt 6:4) to afford the compound **8** as a pink-red solid (0.36 mmol, 80%).

5.1.7. Synthesis of urea derivatives (9a–c): general procedure. Compound **4** (0.45 mmol) was dissolved in dry THF (10 ml). The mixture was placed under agitation and the aryl isocyanate (0.54 mmol) was then added. The reaction mixture was stirred under reflux for 5 h then concentrated under reduced pressure. The solid was filtrated and washed with diethylic ether to give the urea derivatives **9a**–**c**.

5.1.8. Synthesis of acetamide derivatives (10a–c): general procedure. Compound **4** (0.45 mmol), carboxylic acid (0.45 mmol), and TBTU (0.45 mmol) were dissolved in 10 ml of CH_2Cl_2. The reaction mixture was placed under agitation and DIEA (1.35 mmol) was added. The mixture was agitated at room temperature for 24 h. Then, the precipitated solid was filtrated then washed with 10 ml of CH_2Cl_2 to give the acetamide derivatives **10a**–**c**.

5.1.9. Synthesis of 1-hexyl-5-nitro-1*H*-benzimidazole (11a) and 3-hexyl-5-nitro-3*H*-benzimidazole (11b). 5-Nitrobenzimidazole (30.65 mmol) and bromohexane (33.68 mmol) was dissolved in 155 ml of butanone. Potassium carbonate was then added (34.39 mmol). The reaction mixture was stirred under reflux for 24 h then concentrated under reduced pressure and dissolved in ethyl acetate (100 ml). Formed salts were filtrated and the filtrate was concentrated again and dried under vacuum to give a mixture of the required 1-hexyl-5-nitro-1*H*-benzimidazole (**11a**) and its N3 regioisomer (**11b**). Then, this mixture was purified by chromatography on silica gel (AcOEt/hexane 7:3). Two fractions were obtained, one contained the required compound **11a** (16.06 mmol, 54%, $R_f = 0.60$), the other contained the N3 regioisomer **11b** (6.78 mmol, 23%, $R_f = 0.40$).

5.1.10. Synthesis of 1-hexyl-1*H*-benzimidazol-5-amine (13a). Compound **11a** (12.67 mmol) was dissolved in 160 ml of absolute ethanol and $SnCl_2$ dihydrate (64.49 mmol) was then added. The reaction mixture was stirred under reflux for 3 h then concentrated under

reduced pressure and dissolved in 165 ml of ethyl acetate. Sodium bicarbonate (100 ml) was then added. Formed salts were filtrated and washed with 50 ml of AcOEt. The organic phase of the filtrate was washed with water (100 ml), dried on anhydrous sodium sulfate, filtrated, and concentrated under reduced pressure to give an orange red solid. This product was purified by chromatography on silica gel (AcOEt/MeOH 9:1) to afford compound **13a** as a pink solid (5.24 mmol, 41%).

5.1.11. Synthesis of 1-(naphthalen-2-ylmethyl)-5-nitro-1*H*-benzimidazole (12a) and 3-(naphthalen-2-ylmethyl)-5-nitro-3*H*-benzimidazole (12b). 5-Nitrobenzimidazole (30.65 mmol) and bromomethylnaphthalene (33.69 mmol) was dissolved in 155 ml of butanone. Potassium carbonate was then added (34.39 mmol). The reaction mixture was stirred under reflux for 3 h then concentrated under reduced pressure and dissolved in ethyl acetate (100 ml). Formed salts were filtrated and the filtrate was concentrated again and dried under vacuum to give a mixture (orange red solid, 18.03 mmol) of the required compound (**12a**) and its N3 regioisomer (**12b**).

5.1.12. Synthesis of 1-(naphthalen-2-ylmethyl)-1*H*-benzimidazol-5-amine (13b). The mixture containing compounds **12a**–**b** (3.13 mmol) was dissolved in 80 ml of absolute ethanol and $SnCl_2$ dihydrate (15.65 mmol) was then added. The reaction mixture was stirred under reflux for 4 h then concentrated under reduced pressure and dissolved in 85 ml of ethyl acetate. Sodium bicarbonate (100 ml) was then added. Formed salts were filtrated and washed with 50 ml of AcOEt. The organic phase of the filtrate was washed with water (100 ml), dried on anhydrous sodium sulfate, filtrated, and concentrated under reduced pressure to give a mixture (yellow solid, 2.82 mmol) of compound **13b** and its N3 regioisomer. Then, this mixture was purified by chromatography on silica gel (cyclohexane/AcOEt/MeOH 2:7.2:0.8). Two fractions were obtained, one contained the N3 regioisomer (0.58 mmol, 18%, $R_f = 0.78$), the other contained the required compound **13b** (1.06 mmol, 33%, $R_f = 0.44$). The two fractions were pink solids.

5.2. Plasmids

The pPM-LBDhPXR expression plasmid was described previously.[34] The yeast Gal4 DNA binding domain fused to the LBD of hPXR (107–434 aa) was generated from the pPM-LBD using PCR primers that introduced BamHI sites and subcloned into pSG5-puro (gift from Hinrich Gronemeyer, Strasbourg, France).

The pET15b-hPXR expression plasmid was generated by PCR amplification of cDNA-encoding amino acids 107–434 of hPXR using oligonucleotides 5′-CGCGCGCATA TGAAGGAGATGATCATG-3′ and 5′-GCGCGCGG ATCCTCAGCTACCTGTGATGCCG-3′. All plasmids were fully sequenced.

5.3. Generation of stable reporter cell lines

HG_5LN and HGPXR cells were described previously.[35,21,36] Briefly, HG_5LN cells were obtained by integration of a GAL4-responsive gene ($GAL4RE_5$-bGlob-Luc-SV-Neo) in HeLa cells.[36] The HGPXR cell line was obtained by transfecting HG_5LN cells with a plasmid (pSG5-GAL4(DBD)-hPXR(LBD)-puro) which enables the expression of the DNA binding domain of the yeast activator GAL4 (met 1 to ser 147) fused to the ligand-binding domain of hPXR (met 107 to ser 434) and conferes resistance to puromycin. For the strain culture, cells were grown in Dulbecco's modified Eagle's medium (DMEM) containing phenol red and 1 g/l glucose, and supplemented with 5% fetal calf serum (FCS) in a 5% CO_2 humidified atmosphere at 37 °C. HG_5LN cell medium was supplemented with 1 mg/ml geneticin and HGPXR cell medium with 1 mg/ml geneticin and 0.5 μg/ml puromycin.

For tests, cells were grown in DMEM without phenol red, supplemented with 3% dextran-coated charcoal treated fetal calf serum (DCC-FCS).

5.3.1. Living cell luciferase assay. HGPXR and HG_5LN cells were seeded at a density of 5×10^4 cells per well, in 96-well white opaque tissue culture plates (Becton Dickinson) and grown in 200 μl DCC-FCS. Tested compounds were added 24 h later at concentrations between 10 nM and 10 μM and cells were incubated for 16 h with compounds. At the end of incubation, compound containing medium was removed and replaced by 0.3 mM luciferin containing culture medium. Luciferase activity was measured in a MicroBeta Wallac luminometer (EG&G Wallac, Turku, Finland) and luminescence was measured in intact cells for 2 s per well.

5.4. Limited proteolytic digestion

LBD of hPXR in pET-15b expression plasmid (2 μg) was generated by coupled transcription/translation in rabbit reticulocyte lysate using the TNT system according to the manufacturer's instructions (Promega, Madison WI). [^{35}S]Methionine was included in the transcription/translation mix to generate [^{35}S]PXR. Briefly, after a 30-min incubation with ligand at room temperature, hPXR protein was digested at 25 °C with 250 μg/ml trypsin for 10 min. Proteolysis was terminated by adding sodium dodecyl sulfate (SDS) sample buffer and boiling for 10 min. The proteolytic fragments were separated on a 12% SDS–polyacrylamide gel. Gels were dried and radio-labeled digestion products were visualized by autoradiography using a bio-imaging analyzer (Fujix BAS1000 Phosphorimager). Autoradiograms were analyzed using an image analyzing software. Experiments were performed three times. To determine the protection of hPXR by a test compound, the intensity of the 30 kDa band of hPXR-LBD treated with ligand was divided by the intensity of the 30 kDa of hPXR treated by ethanol. The protection value in presence of ethanol was thus taken as 1.

5.5. Data analysis and statistics

In the transactivation assay, each compound was tested at various concentrations in at least three separate

experiments in triplicate wells and data are presented as means ± SD. HG_5LN cells assessed us to evaluate hPXR-independent luciferase expression as well as the toxicity of the compounds. HGPXR cells were designed to detect hPXR agonists. Individual agonist dose–response curves on these cells were fitted using the sigmoidal dose–response function of a graphics and statistics software (Graph-Pad Prism, version 4.0, 2003, Graphpad Software Incorporated, San Diego, CA). EC_{50}, effective concentration for half-maximal luciferase activity was calculated via nonlinear regression. This equation was used to fit the data in the graphic software. Transactivation data are presented as EC_{50} values for each compound tested.

In the proteolysis assay, **C2BA-4**, **6c**, **6m**, and **6n** were tested at various concentrations in at least three separate experiments in triplicate wells and data are presented as means ± SD. HG_5LN cells assessed us to evaluate hPXR-independent luciferase expression as well as the toxicity of the compounds. HGPXR cells were designed to detect hPXR agonists. Individual agonist dose–response curves on these cells were fitted using the sigmoidal dose–response function of a graphics and statistics software (Graph-Pad Prism, version 4.0, 2003, Graphpad Software Incorporated, San Diego, CA). EC_{50}, effective concentration for half-maximal luciferase activity was calculated via nonlinear regression. This equation was used to fit the data in the graphic software. Transactivation data are presented as EC_{50} values for each compound tested.

One-way analysis of variance (ANOVA) was used to demonstrate statistical difference between the activity percentage of control and tested compounds with the help of GraphPad Prism software (GraphPad, San Diego, CA). Calculation of statistical significance (P values <0.05) between treated and controlled groups were performed using Tukey's post hoc test.

5.6. Liver samples, hepatocyte cultures and treatment

Hepatocytes were prepared from lobectomy segments resected from adult patients for medical purposes unrelated to our research program. The use of these human hepatic specimens for scientific purposes has been approved by the French National Ethics Committee.

Human hepatocytes were prepared and cultured as previously described.[37] Cells were plated into collagen-coated P12 dishes at 0.17×10^{-6} cells/cm^2 in a hormonally and chemically defined medium consisting of a mixture of Williams' E and Ham's F-12 (1:1 v/v). Treatment with 10^{-6} M and 10^{-5} M effector solutions or solvent (DMSO 0.1%) started 48 h after plating and lasted 24 h.

5.6.1. Total RNA purification and CYP3A4 quantitative PCR. Total RNA was isolated with TRIzol reagent (Invitrogen). cDNA was synthetized from 1 μg of total RNA using the SuperScript-II First-Strand Synthesis System (Invitrogen) for RT-PCR at 42 °C for 60 min in the presence of random hexamers (Invitrogen), and then 10-fold diluted in water. Two microliters was used in duplicates for quantitative PCR amplification of CYP2B6, CYP3A4, and β-actin, as internal control, using the Light Cycler apparatus (Roche Diagnostic Corporation, Meylan, France). The following program was used: denaturation step at 95 °C for 10 min, 45 cycles PCR (denaturation at 95 °C for 10 s, annealing at 65 °C for 8 s, elongation at 65 °C for 15 s). Sense and reverse primers, respectively, were as follows: β-actin: 5′-tgggcatggtgcagaaggat and 5′-tccatcacgatgccagtggt; CYP3A4: 5′-cacaaaccggaggccttttg and 5′-atccatgctgtagggccccaa; CYP2B6: 5′-ggccatacgggaggcccttg and 5′-agggcccttggatttccg and GAPDH: 5′-ggtcggagtcaacggatttggtcg and 5′-caaagttgtcatggatgacc. The curves of amplification were read with the Roche's Light Cycler Software using the comparative cycle threshold (C_t) method. Relative quantifications of the target mRNAs were calculated after normalization of C_ts with respect to the GAPDH levels. Values are expressed as fold induction compared to non-treated cells (DMSO 0.1%) ± SD.

5.7. In silico modeling: docking of 6n to the crystal structure using Surflex-2.1

Protein preparation for surflex docking was done in Sybyl 7.3 (Tripos Inc., St. Louis, MO). From the Protein Databank entry 2O9I, the chain A, Gly142-Gly433, was chosen for a protein site preparation and water molecules were deleted. Only hydrogen position energy optimization was performed after addition of hydrogen atoms, then ligand **T0901317** was removed and saved in mol2 format. The resulting protein was saved in Tripos mol2 format. A ligand-based approach with **T0901317** as ligand was performed to generate the binding site (protomol) as follows: surflex-dock –adapt_proto –adapt_thresh 0.4 proto. Compound **6n** in mol2 format was docked into the protomol using the –pgeom option and with or without restraints. For the restrained docking process the *N*-phenyl-benzenesulfonamide moiety of **T0901317** was used as placed fragment. For both strategies, scores obtained for the 20 docking poses were from 4.8 to 6.3.

Acknowledgments

This study has been partly supported by the European Union Network CASCADE (FOOD-CT-2003-506319) and ANR JCJC-05-47810 (J.-M.P). C.B. is a recipient of the MENRT from the French Government. V.N. is a recipient of the French Young Researcher Program (INSERM). The authors Drs. Adrien Cavé and Andre Padilla for NMR assistance. We are also grateful to Mr. Terry Page and Dr. Julien Viaud for the critical reading of this manuscript. This work was sponsored by the CNRS and INSERM.

Supplementary data

Data for the superimposition of **6n** with the *N*-phenyl-benzenesulfonamide fragment of **T0901317**. The activity of **T0901317** and other ligands on reporter cell system;

SDS–PAGE electrophoresis showing the Limited Proteolytic digestion in presence of ligands; table providing results from purity analyses by HPLC for key target compounds and chemical shifts of synthesized compounds; This material is available via the Internet at www.sciencedirect.com. Supplementary data associated with this article can be found, in the online version, at doi:10.1016/j.bmc.2008.02.020.

References and notes

1. Lehmann, J. M.; McKee, D. D.; Watson, M. A.; Willson, T. M.; Moore, J. T.; Kliewer, S. A. *J. Clin. Invest.* **1998**, *102*, 1016–1023.
2. Blumberg, B.; Sabbagh, W., Jr.; Juguilon, H.; Bolado, J., Jr.; van Meter, C. M.; Ong, E. S.; Evans, R. M. *Gene Dev.* **1998**, *12*, 3195–3205.
3. Bertilsson, G.; Heidrich, J.; Svensson, K.; Asman, M.; Jendeberg, L.; Sydow-Backman, M.; Ohlsson, R.; Postlind, H.; Blomquist, P.; Berkenstam, A. *Proc. Natl. Acad. Sci. U.S.A.* **1998**, *95*, 12208–12213.
4. Xie, W.; Barwick, J. L.; Simon, C. M.; Pierce, A. M.; Safe, S.; Blumberg, B.; Guzelian, P. S.; Evans, R. M. *Gene Dev.* **2000**, *14*, 3014–3023.
5. Kast, H. R.; Goodwin, B.; Tarr, P. T.; Jones, S. A.; Anisfeld, A. M.; Stoltz, C. M.; Tontonoz, P.; Kliewer, S.; Willson, T. M.; Edwards, P. A. *J. Biol. Chem.* **2002**, *277*, 2908–2915.
6. Kliewer, S. A.; Goodwin, B.; Willson, T. M. *Endocr. Rev.* **2002**, *23*, 687–702.
7. Goodwin, B.; Hodgson, E.; Liddle, C. *Mol. Pharmacol.* **1999**, *56*, 1329–1339.
8. Staudinger, J.; Liu, Y.; Madan, A.; Habeebu, S.; Klaassen, C. D. *Drug Metab. Dispos.* **2001**, *29*, 1467–1472.
9. Zollner, G.; Marschall, H. U.; Wagner, M.; Trauner, M. *Mol. Pharm.* **2006**, *3*, 231–251.
10. Matic, M.; Mahns, A.; Tsoli, M.; Corradin, A.; Polly, P.; Robertson, G. R. *Int. J. Biochem. Cell Biol.* **2007**, *39*, 478–483.
11. Orans, J.; Teotico, D. G.; Redinbo, M. R. *Mol. Endocrinol.* **2005**, *19*, 2891–2900.
12. Lamba, V.; Yasuda, K.; Lamba, J. K.; Assem, M.; Davila, J.; Strom, S.; Schuetz, E. G. *Toxicol. Appl. Pharmacol.* **2004**, *199*, 251–265.
13. Xie, W.; Yeuh, M. F.; Radominska-Pandya, A.; Saini, S. P.; Negishi, Y.; Bottroff, B. S.; Cabrera, G. Y.; Tukey, R. H.; Evans, R. M. *Proc. Natl. Acad. Sci. U.S.A.* **2003**, *100*, 4150–4155.
14. Stedman, C. A.; Liddle, C.; Coulter, S. A.; Sonoda, J.; Alvarez, J. G.; Moore, D. D.; Evans, R. M.; Downes, M. *Proc. Natl. Acad. Sci. U.S.A.* **2005**, *102*, 2063–2068.
15. Wright, M. C. *Biochem. Soc. Trans.* **2006**, *34*, 1119–1123.
16. Zhou, J.; Zhai, Y.; Mu, Y.; Gong, H.; Uppal, H.; Toma, D.; Ren, S.; Evans, R. M.; Xie, W. *J. Biol. Chem.* **2006**, *281*, 15013–15020.
17. Jones, S. A.; Moore, L. B.; Shenk, J. L.; Wisely, G. B.; Hamilton, G. A.; McKee, D. D.; Tomkinson, N. C.; LeCluyse, E. L.; Lambert, M. H.; Willson, T. M.; Kliewer, S. A.; Moore, J. T. *Mol. Endocrinol.* **2000**, *14*, 27–39.
18. Lemaire, G.; Benod, C.; Nahoum, V.; Pillon, A.; Boussioux, A. M.; Guichou, J. F.; Subra, G.; Pascussi, J. M.; Bourguet, W.; Chavanieu, A.; Balaguer, P. *Mol. Pharmacol.* **2007**.
19. Matassa, V. G.; Brown, F. J.; Bernstein, P. R.; Shapiro, H. S., ; Maduskuie, T. P., Jr.; Cronk, L. A.; Vacek, E. P.; Yee, Y. K.; Snyder, D. W.; Krell, R. D., et al. *J. Med. Chem.* **1990**, *33*, 2621–2629.
20. Matsoukas, J. M.; Panagiotopoulos, D.; Keramida, M.; Mavromoustakos, T.; Yamdagni, R.; Wu, Q.; Moore, G. J.; Saifeddine, M.; Hollenberg, M. D. *J. Med. Chem.* **1996**, *39*, 3585–3591.
21. Lemaire, G.; Mnif, W.; Pascussi, J. M.; Pillon, A.; Rabenoelina, F.; Fenet, H.; Gomez, E.; Casellas, C.; Nicolas, J. C.; Cavailles, V.; Duchesne, M. J.; Balaguer, P. *Toxicol. Sci.* **2006**, *91*, 501–509.
22. Lemaire, G.; de Sousa, G.; Rahmani, R. *Biochem. Pharmacol.* **2004**, *68*, 2347–2358.
23. Xue, Y.; Moore, L. B.; Orans, J.; Peng, L.; Bencharit, S.; Kliewer, S. A.; Redinbo, M. R.; Xue, Y.; Chao, E.; Zuercher, W. J.; Willson, T. M.; Collins, J. L.; Redinbo, M. R. *Mol. Endocrinol.* **2007**, *21*, 1028–1038.
24. Chrencik, J. E.; Orans, J.; Moore, L. B.; Xue, Y.; Peng, L.; Collins, J. L.; Wisely, G. B.; Lambert, M. H.; Kliewer, S. A.; Redinbo, M. R. *Mol. Endocrinol.* **2005**, *19*, 1125–1134.
25. Watkins, R. E.; Davis-Searles, P. R.; Lambert, M. H.; Redinbo, M. R. *J. Mol. Biol.* **2003**, *331*, 815–828.
26. Watkins, R. E.; Maglich, J. M.; Moore, L. B.; Wisely, G. B.; Noble, S. M.; Davis-Searles, P. R.; Lambert, M. H.; Kliewer, S. A.; Redinbo, M. R. *Biochemistry* **2003**, *42*, 1430–1438.
27. Xue, Y.; Chao, E.; Zuercher, W. J.; Willson, T. M.; Collins, J. L.; Redinbo, M. R. *Bioorg. Med. Chem.* **2007**, *15*, 2156–2166.
28. Moras, D.; Gronemeyer, H. *Curr. Opin. Cell Biol.* **1998**, *10*, 384–391.
29. Watkins, R. E.; Wisely, G. B.; Moore, L. B.; Collins, J. L.; Lambert, M. H.; Williams, S. P.; Willson, T. M.; Kliewer, S. A.; Redinbo, M. R. *Science* **2001**, *292*, 2329–2333.
30. Jain, A. N. *J. Med. Chem.* **2003**, *46*, 499–511.
31. Jain, A. N. *J. Comput. Aided Mol. Des.* **2007**, *21*, 281–306.
32. Lamba, J.; Lamba, V.; Schuetz, E. *Curr. Drug Metab.* **2005**, *6*, 369–383.
33. Langmade, S. J.; Gale, S. E.; Frolov, A.; Mohri, I.; Suzuki, K.; Mellon, S. H.; Walkley, S. U.; Covey, D. F.; Schaffer, J. E.; Ory, D. S. *Proc. Natl. Acad. Sci. U.S.A.* **2006**, *103*, 13807–13812.
34. Ourlin, J. C.; Lasserre, F.; Pineau, T.; Fabre, J. M.; Sa-Cunha, A.; Maurel, P.; Vilarem, M. J.; Pascussi, J. M. *Mol. Endocrinol.* **2003**, *17*, 1693–1703.
35. Balaguer, P.; Boussioux, A. M.; Demirpence, E.; Nicolas, J. C. *Luminescence* **2001**, *16*, 153–158.
36. Seimandi, M.; Lemaire, G.; Pillon, A.; Perrin, A.; Carlavan, I.; Voegel, J. J.; Vignon, F.; Nicolas, J. C.; Balaguer, P. *Anal. Biochem.* **2005**, *344*, 8–15.
37. Pascussi, J. M.; Gerbal-Chaloin, S.; Fabre, J. M.; Maurel, P.; Vilarem, M. J. *Mol. Pharmacol.* **2000**, *58*, 1441–1450.